

## ABC-Type *meso*-Triaryl-Substituted Subporphyrins

Kota Yoshida,<sup>[a]</sup> Hirotaka Mori,<sup>[a]</sup> Takayuki Tanaka,<sup>[a]</sup> Tadashi Mori,<sup>\*[b]</sup> and Atsuhiko Osuka<sup>\*[a]</sup>

**Keywords:** Synthetic methods / Porphyrinoids / Chirality / Conformational analysis

ABC-Type subporphyrins **5a–5h**, which bear three different *meso*-aryl substituents, were rationally synthesized by condensation of AB-type tripyrranes and aroyl chlorides. ABC-Type subporphyrins **5i** and **5j** were synthesized by Pd-catalyzed amination reaction of 4-bromophenyl subporphyrins **5e** and **5h**, respectively. Comparative studies on these ABC-type subporphyrins with A<sub>3</sub>-type subporphyrins and A<sub>2</sub>B-type subporphyrins revealed that substituent effects are mostly simple superpositions of individual substituents but cooperative effects are recognized for subporphyrins which bear both

electron-donating and electron-withdrawing substituents. Despite extensive attempts, enantiomeric separation of B-methoxy ABC-type subporphyrins was unsuccessful, whereas B-phenylated ABC-type subporphyrins were separated to pure enantiomers. Separated enantiomers showed weak but distinct CD signals reflecting the chiral clockwise/anticlockwise arrangements of the *meso*-aryl substituents. These results suggest facile racemization through S<sub>N</sub>1-type heterolysis of the B–OMe bond in solution.

### Introduction

Subporphyrins are ring-contracted porphyrins that consist of three regularly connected pyrroles and three methine carbons encompassing a 14π-aromatic electronic network.<sup>[1]</sup> Following our first report of the synthesis of tribenzosubporphyrins in 2006,<sup>[2]</sup> Kobayashi and ourselves reported independently the synthesis of A<sub>3</sub>-type *meso*-triaryl-substituted subporphyrins.<sup>[3,4]</sup> Different from *meso*-aryl-substituted porphyrins, *meso*-aryl-substituted subporphyrins experience remarkably large substituent effects on optical and electronic properties owing to negligible rotational barriers of *meso*-aryl substituents.<sup>[5]</sup> Quite recently, we developed a stepwise synthetic route to A<sub>2</sub>B-type *meso*-triarylsbporphyrins through an A<sub>2</sub>-type tripyrrane precursor.<sup>[6]</sup> Such A<sub>2</sub>B-type subporphyrins were also prepared by transition-metal-catalyzed cross-coupling reactions of *meso*-bromo-substituted subporphyrins.<sup>[7]</sup> In this paper, we report the synthesis of ABC-type *meso*-triaryl-substituted subporphyrins through condensation of AB-type tripyrranes and aroyl chlorides. ABCD-type porphyrins possessing four different *meso*-aryl groups have been prepared through an elegant route developed by Lindsey et al.<sup>[8]</sup> However, these molecules are usually achiral as a result of a plane of symmetry.

In contrast, subporphyrins adopt domed, bowl-like structures, which leads to a situation whereby ABC-type subporphyrins are chiral, given no flip-flop bowl inversion. Whereas enantiomeric separation of B-methoxy ABC-type subporphyrins has been unsuccessful, B-phenylated ABC-type subporphyrins have been separated into each enantiomerically pure form.

### Results and Discussion

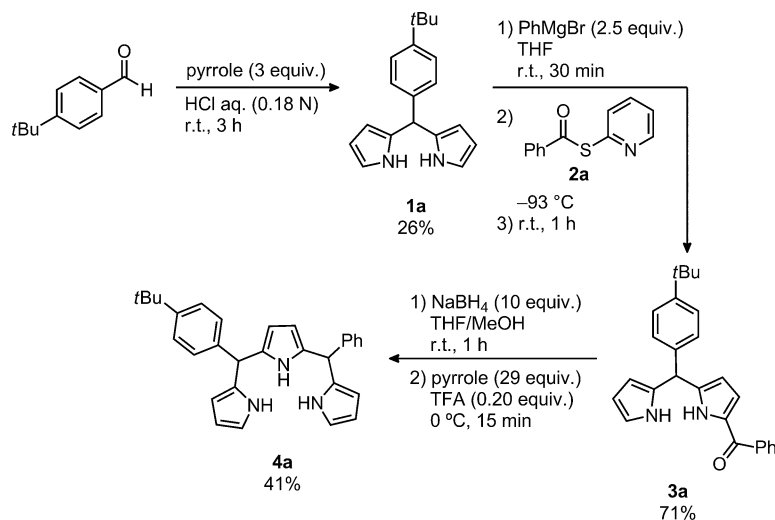
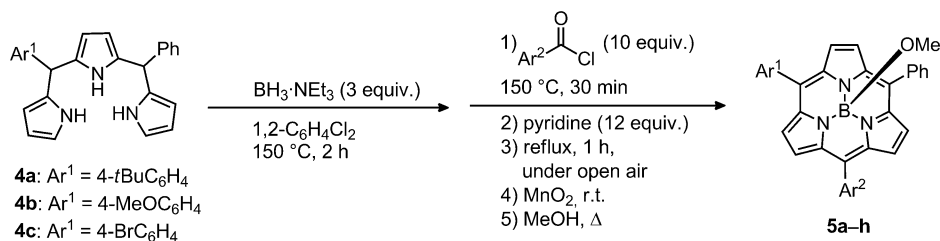
#### Synthesis

In the present synthesis, nonsymmetrical AB-type tripyrrmethanes were used as key precursors of ABC-type *meso*-triaryl subporphyrins. 5-(4-*tert*-Butylphenyl)-10-phenyltripyrane (**4a**) was prepared as shown in Scheme 1. 1-Benzoyl-5-(4-*tert*-butylphenyl)dipyrrromethane (**3a**) was prepared with an existing procedure by using phenylmagnesium bromide instead of ethylmagnesium bromide.<sup>[8f]</sup> Benzoyl dipyrrromethane **3a** was reduced with NaBH<sub>4</sub> and then reacted with pyrrole to furnish the AB-type tripyrrane **4a**.<sup>[7]</sup> In a similar manner, 5-(4-methoxyphenyl)-10-phenyltripyrane (**4b**) and 5-(4-bromophenyl)-10-phenyltripyrane (**4c**) were prepared. AB-type tripyrranes **4a–4c** were converted into their borane–triethylamine complexes, which were then condensed with 10 equiv. of the appropriate aroyl chlorides under previously reported conditions.<sup>[6]</sup> Fractions of subporphyrin and subchlorin that were eluted closely in column chromatography were collected and subjected to oxidation with activated MnO<sub>2</sub> to convert subchlorin into subporphyrin. Then, the axial ligand was quantitatively converted into the methoxy group by stirring a solution of sub-

[a] Department of Chemistry, Graduate School of Science, Kyoto University, Sakyo-ku, Kyoto 606-8502, Japan  
E-mail: osuka@kuchem.kyoto-u.ac.jp

[b] Department of Applied Chemistry, Graduate School of Engineering, Osaka University, 2-1 Yamada-oka, Suita 565-0871, Japan  
E-mail: tmori@chem.eng.osaka-u.ac.jp

Supporting information for this article is available on the WWW under <http://dx.doi.org/10.1002/ejoc.201402435>.

Scheme 1. Synthesis of the AB-type tripyrromethane **4a**.Scheme 2. Synthesis of the ABC-type subporphyrins **5a–5h**.Table 1. ABC-type subporphyrins **5a–5h**.

Product	Ar <sup>1</sup>	Ar <sup>2</sup>	Yield [%]
<b>5a</b>			7.5
<b>5b</b>			6.9
<b>5c</b>			5.8
<b>5d</b>			12
<b>5e</b>			12
<b>5f</b>			24
<b>5g</b>			3.2
<b>5h</b>			12

porphyrin in dichloromethane and methanol at 50 °C for about 15 min. Repeated separations by silica gel column chromatography gave subporphyrins **5a–5h** in 3.2–24% isolated yields (Scheme 2 and Table 1). Subporphyrins **5i** and **5j** were synthesized by Pd-catalyzed amination reaction of subporphyrins **5e** and **5h** in 38 and 50% yields, respectively (Scheme 3 and Table 2).

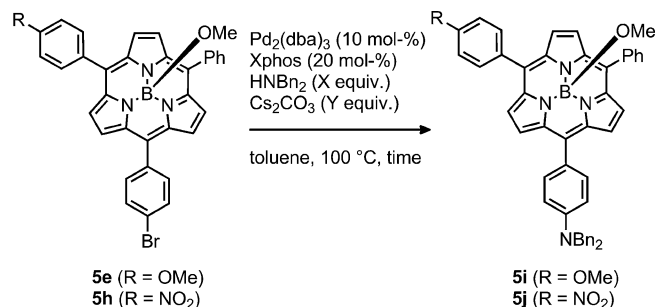
Scheme 3. Synthesis of the ABC-type subporphyrins **5i** and **5j**.

Table 2. Reaction conditions for Pd-catalyzed amination reaction.

Product	X (equiv.)	Y (equiv.)	Time	Yield [%]
<b>5i</b>	2.0	2.0	2 d	38
<b>5j</b>	1.2	1.4	10 h	50

## X-ray Crystallographic Analyses

The structures of subporphyrins **5g**, **5h**, **5i**, and **5j** were determined by single-crystal X-ray diffraction analysis. All subporphyrins show bowl-shaped structures with bowl depths (defined by the distance from the central boron atom to the mean plane of the peripheral six  $\beta$ -carbons) of 1.33, 1.32, 1.35, and 1.29 Å, respectively. The phenyl and 2-thienyl groups in **5g** are severely disordered in the crystal structure and all three *meso*-aryl groups are also severely disordered in the crystal structure of **5h**, whereas such disorder is not observed for the crystals of **5i** and **5j**. The dihedral angle of the 2-thienyl substituent toward the subporphyrin core in **5g** is small (37.5°), which is similar to the reported tri(2-thienyl)-substituted subporphyrin and related molecules.<sup>[9]</sup> The 4-(dibenzylamino)phenyl groups in **5i** and **5j** both display a characteristic structural distortion toward the quinonoidal form and small dihedral angles (38.7° and 33.4°, respectively), as observed for *meso*-(4-dibenzylaminophenyl)-substituted subporphyrins.<sup>[5b]</sup> The crystal structure of **5i** was found as a racemate and the enantiomers have their concave faces facing each other in an offset manner with the concave face of the adjacent subporphyrin filled by the dibenzylamino group (Figure 1, b).

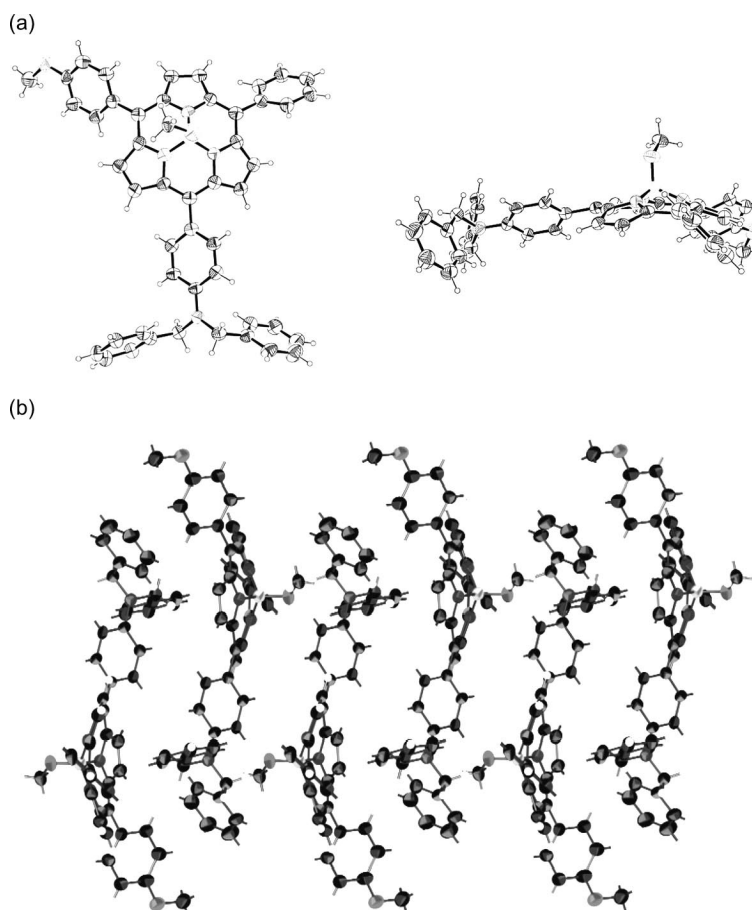


Figure 1. (a) X-ray crystal structure of **5i**. (b) A view of the crystal packing of subporphyrin **5i**. Thermal ellipsoids represent 30% probability.

## <sup>1</sup>H NMR Spectra

The <sup>1</sup>H NMR spectra of the ABC-type subporphyrins **5a–5j** should exhibit six doublet peaks owing to the pyrrolic  $\beta$ -protons, reflecting the nonequivalent chemical shifts arising from their  $C_1$  symmetry. Nevertheless, in most cases, it is hard to distinguish all six doublet peaks owing to severe overlap of the signals. However, the <sup>1</sup>H NMR spectrum of subporphyrin **5a** has six distinct doublet peaks owing to the  $\beta$ -protons at room temperature as shown in Figure 2. H–H scalar coupling correlation has been revealed by COSY measurement (see Figure S10 in the Supporting Information).

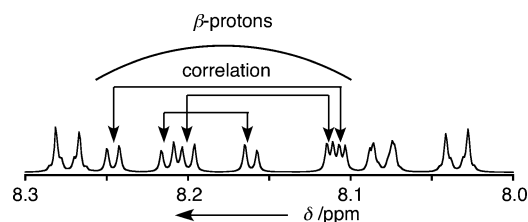


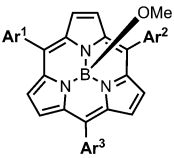
Figure 2. <sup>1</sup>H NMR spectrum of subporphyrin **5a** in CDCl<sub>3</sub> at room temperature.

## Absorption and Fluorescence Spectra

The UV/Vis absorption and fluorescence spectral data of subporphyrins **5a–5j** are listed in Table 3 and UV/Vis absorption and fluorescence spectra of some of the subporphyrins are shown in Figure 3.

In the absorption spectra of  $A_3$ -type *meso*-triaryl subporphyrins, the 4-nitrophenyl group, 2-thienyl group, and 4-aminophenyl group are known to exert strong substituent effects on the optical properties of subporphyrins.<sup>[4,5b,9]</sup> This is also valid for the present ABC-type subporphyrins, because when one of these substituents is present, subporphyrins exhibit perturbed absorption and fluorescence spectra similar to those of the corresponding  $A_3$ -type subporphyrins. The absorption spectra of subporphyrins **5a**, **5c**, and **5h** that bear a 4-nitrophenyl substituent display Soret-like bands at 380, 383, and 380 nm, and Q-like bands at 466 and 495 nm, 467 and 498 nm, and 464 and 493 nm, respectively. The red shifts of Soret-like bands in **5a**, **5c**, and **5h** relative to triphenylsubporphyrin **7a** are smaller than

Table 3. Optical properties of subporphyrins **5a–5j** and **7a–7f**.

				$\lambda_{\text{em}}^{[d]}$ [nm]	$\Phi_{\text{F}}^{[d]}$
	$\lambda_{\text{abs}}$ [nm] ( $\epsilon$ [ $10^4 \text{ M}^{-1} \text{ cm}^{-1}$ ])	$\lambda_{\text{em}}^{[d]}$ [nm]	$\Phi_{\text{F}}^{[d]}$		
<b>5a</b>	380 (6.3)	466 (0.8)	495 (0.9)	598	0.03
<b>5b</b>	377 (16.9)	46 (1.1)	491 (1.2)	529	0.14
<b>5c</b>	383 (8.3)	467 (1.1)	498 (1.3)	602	0.01
<b>5d</b>	379 (16.2)	464 (1.3)	491 (1.3)	533	0.18
<b>5e</b>	376 (16.3)	462 (1.2)	489 (1.2)	528	0.05
<b>5f</b>	378 (17.4)	463 (1.3)	491 (1.4)	533	0.19
<b>5g</b>	382 (13.6)	470 (1.0)	501 (1.3)	556	0.15
<b>5h</b>	380 (9.9)	464 (1.2)	493 (1.2)	574	0.06
<b>5i</b>	357 (4.8)	390 (9.0)	470 (1.0) 506 (2.0)	595	0.60
<b>5j</b>	360 (4.0)	407 (5.5)	512 (1.8)	603	< 0.01
<b>7a</b> <sup>[a]</sup>	373 (16.6)	461 (1.3)	484 (0.9)	516	0.14
<b>7b</b> <sup>[a]</sup>	397 (11.1)	471 (1.8)	492 (1.6)	543	0.15
<b>7c</b> <sup>[b]</sup>	394 (11.9)	522 (1.7)		603	0.35
<b>7d</b> <sup>[c]</sup>	359 (5.6)	394 (8.9)	505 (2.1)	605	0.59
<b>7e</b> <sup>[c]</sup>	343 (3.0)	401 (12.4)	518 (2.8)	622	0.60
<b>7f</b> <sup>[c]</sup>	401 (15.4)	527 (3.5)		633	0.58

[a] See ref.<sup>[4]</sup>. [b] See ref.<sup>[9]</sup>. [c] See ref.<sup>[5b]</sup>. [d] Excited at the peak top of each Soret band.

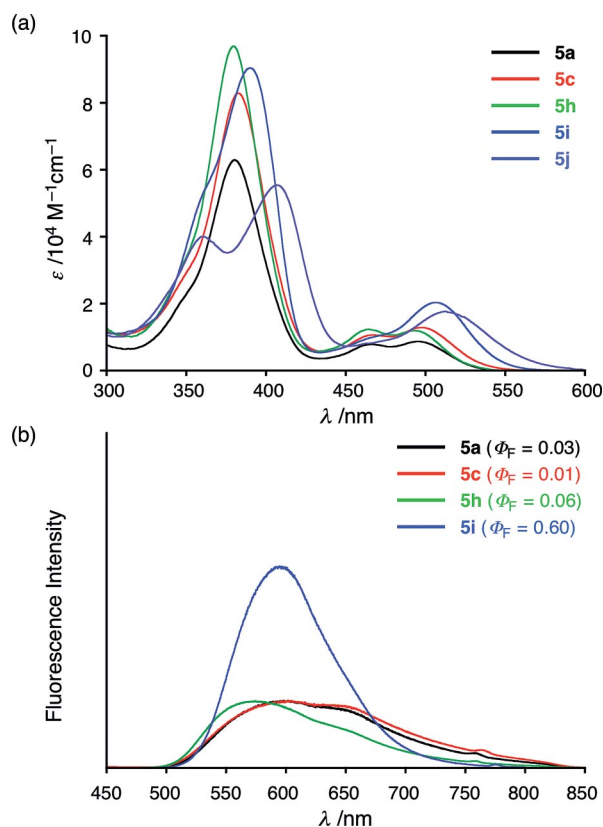


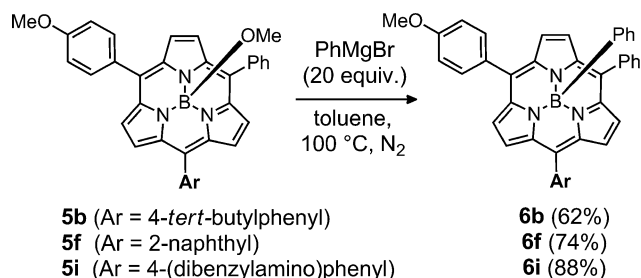
Figure 3. (a) UV/Vis absorption spectra of subporphyrins **5a**, **5c**, **5h**, **5i**, and **5j** in  $\text{CH}_2\text{Cl}_2$ . (b) Fluorescence spectra of subporphyrins **5a**, **5c**, **5h**, and **5i** in  $\text{CH}_2\text{Cl}_2$ .

that of tri(4-nitrophenyl) subporphyrin **7b**, whereas the corresponding red shifts in Q-like bands are similar. Subporphyrin **7b** exhibits a fluorescence peak at 543 nm with moderate fluorescence quantum yields ( $\Phi_{\text{F}} = 0.15$ ) in  $\text{CH}_2\text{Cl}_2$ . In contrast, subporphyrins **5a** and **5c** emit reddish-orange fluorescence with peaks at 598 and 602 nm and long tails that extend out to over 800 nm with small fluorescence quantum yields ( $\Phi_{\text{F}} = 0.03$  and 0.01) in  $\text{CH}_2\text{Cl}_2$ . A possible explanation for this phenomenon is the different degree of intramolecular electron transfer from the subporphyrin  $S_1$ -state to the *meso*-4-nitrophenyl group, which is supposed to trigger a red shift for fluorescence and fluorescence quenching. When the subporphyrin core becomes more electron-rich, the influence of the 4-nitrophenyl substituent becomes more important. Observed larger red shifts of the Q-bands and stronger fluorescence quenching in subporphyrins **5a** and **5c** relative to **7b** and **5h** (the fluorescence peak at 574 nm and  $\Phi_{\text{F}} = 0.06$ ) can be accounted for in this way. As a similar feature, the absorption spectrum of subporphyrin **5i** is slightly different from that of mono[(4-dibenzylamino)phenyl]-substituted subporphyrin **7d**. Namely, the Soret-like band of subporphyrin **5i** has a peak at 390 nm and a shoulder at 357 nm, whereas that of subporphyrin **7d** has two peaks at 359 and 394 nm. The fluorescence spectrum of **5i** is less red-shifted than that of subporphyrin **7d**. It seems likely that the substituent effect of the *meso*-(4-dibenzylamino)phenyl group is slightly attenuated by the

electron-donating *meso*-(4-methoxy)phenyl group in **5i**. In contrast, the absorption spectrum of subporphyrin **5j** that bears both electron-donating and accepting substituents shows two Soret-like peaks at 360 and 407 nm, and is actually non-fluorescent ( $\Phi_F < 0.01$ ) and its fluorescence peak is red-shifted to 603 nm. These observations strongly suggest that the substituent effect of the 4-nitrophenyl group is not simply additive but can be enhanced in combination with other electron-donating *meso*-substituents.

### Enantiomeric Separations

ABC-Type subporphyrins should be chiral, providing that there is no flip-flop bowl inversion. This molecular chirality is classified as bowl chirality,<sup>[10]</sup> which is seen for subphthalocyanine,<sup>[11]</sup> sumanene,<sup>[12]</sup> fullerene<sup>[13]</sup> and carbon nanotube systems.<sup>[14]</sup> Studies on bowl chirality have been extensively explored, because such three-dimensional chiral  $\pi$ -surfaces can serve as an important motif for molecular recognition and asymmetric catalysis. We thus attempted enantiomeric separation of the ABC-type subporphyrins prepared in this study. However, we failed in our attempts to resolve the enantiomers of B-methoxy ABC-type subporphyrins despite extensive efforts with various chiral columns and eluting solvent systems. Then, it was suspected that racemization of B-methoxy ABC subporphyrins might be triggered by a facile flip-flop bowl inversion that might be possible through  $S_N1$ -type heterolysis. We envisaged that such heterolysis would be difficult for B-phenyl



Scheme 4. Synthesis of subporphyrins **6b**, **6f**, and **6i** that bear a B-phenyl group through reaction with Grignard reagents.

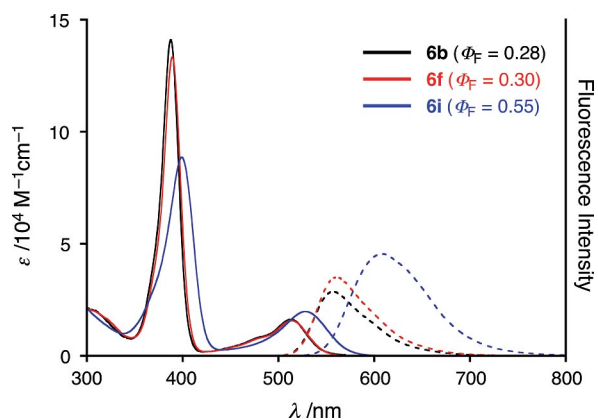
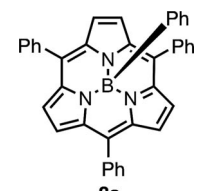


Figure 4. UV/Vis absorption and fluorescence spectra of subporphyrins **6b**, **6f**, and **6i** in  $\text{CH}_2\text{Cl}_2$ .

subporphyrins and thus we converted B-methoxy subporphyrins **5b**, **5f**, and **5i** into the corresponding B-phenylated subporphyrins **6b**, **6f**, and **6i**, respectively, by B-arylation reaction with phenylmagnesium bromide<sup>[15]</sup> (Scheme 4). The UV/Vis absorption spectra and fluorescence spectra of subporphyrins **6b**, **6f**, and **6i** are shown in Figure 4 and the relevant data are listed in Table 4.

Table 4. Optical properties of subporphyrins **6b**, **6f**, **6i**, and **8a**.



**8a**

	$\lambda_{\text{abs}}$ [nm] ( $\epsilon$ [ $10^4 \text{ M}^{-1} \text{ cm}^{-1}$ ])			$\lambda_{\text{em}}$ [nm] <sup>[b]</sup>	$\Phi_F$ <sup>[b]</sup>
<b>6b</b>	388 (14.0)	478 (0.8)	512 (1.6)	558	0.28
<b>6f</b>	389 (13.0)	479 (0.8)	513 (1.6)	561	0.30
<b>6i</b>	399 (8.9)	538 (2.0)		608	0.55
<b>8a</b> <sup>[a]</sup>	385 (13.6)	478 (0.9)	507 (1.3)	541	0.16

[a] See ref.<sup>[15]</sup>. [b] Excited at the peak top of each Soret band.

The absorption and fluorescence spectra of subporphyrins **6b** and **6f** are red-shifted relative to those of subporphyrins **5b** and **5f**, as for subporphyrin **8a**. The Soret-like band of **6i** has a single peak at 399 nm probably as a consequence of attenuation of the substituent effect of the 4-(dibenzylamino)phenyl group, because the subporphyrin core is less electron-deficient owing to the electron-donating B-phenyl group. The fluorescence quantum yields of **6b** and **6f** are larger than those of **5b** and **5f**, whereas that of **6i** is slightly lower than that of **5i**. We were delighted to see that the bands of the two enantiomers could be resolved by a chiral HPLC column (Figure 5). Under these conditions,

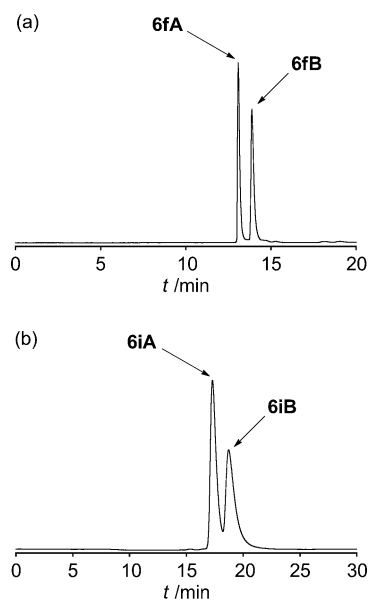


Figure 5. Chiral HPLC chromatographic chart of (a) **6f** and (b) **6i** (column: CHIRALPAK<sup>®</sup> IB-3; eluent: THF/*n*-hexane, 5:95; flow rate: 2.5 mL/min).

the enantiomeric separations of **6f** and **6i** to **6fA** and **6fB**, and to **6iA** and **6iB**, respectively, have been successfully accomplished. However, the enantiomeric separation of **6b** has not been accomplished. All the separated enantiomers did not undergo racemization even after being heated to reflux for 12 h in toluene, indicating their structural robustness. Enantiomers **6fA** and **6fB**, and **6iA** and **6iB** display exactly the same  $^1\text{H}$  NMR, UV/Vis, and fluorescence spectra but different circular dichroism (CD) spectra (see the Supporting Information). Unfortunately, these CD spectra were extremely weak, probably because the chirality arises not from the subporphyrin core but mainly comes from the chiral arrangement of the peripheral aryl substituents. In addition, there are 8 possible conformers with regard to the *meso*-aryl substituents (*R* or *S* as defined in the Supporting Information) and each conformer shows quite different Cotton effects, which leads to near cancelation. This effect was fairly well reproduced by our simulation of the CD spectrum of **6f**, in which the conformer population was weighted by Boltzmann distribution (see Figure S14 in the Supporting Information).

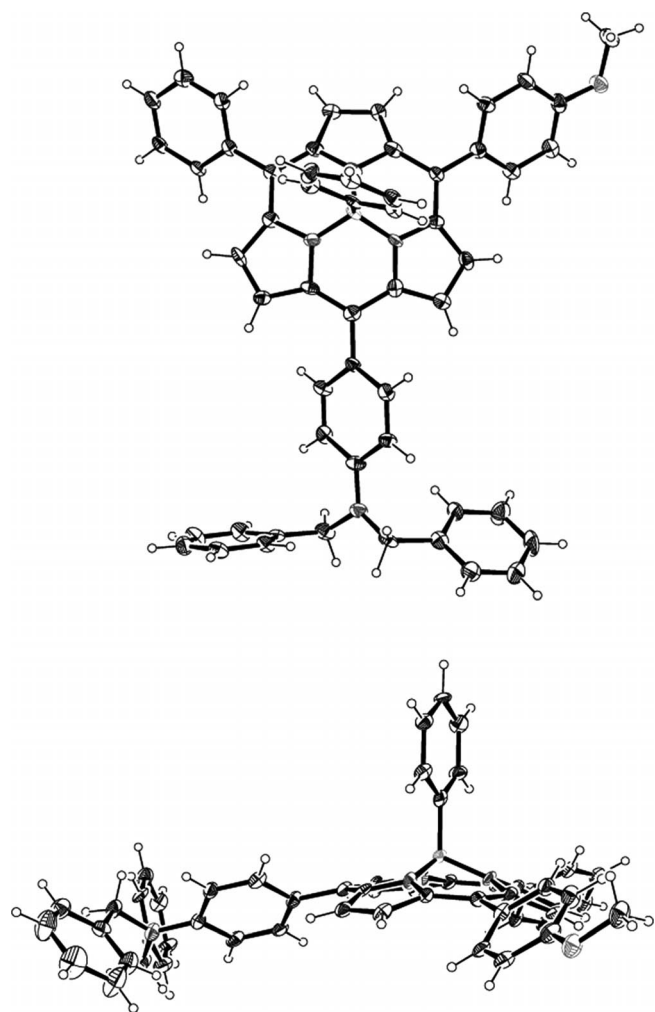


Figure 6. X-ray crystal structure of subporphyrin **6iB**. Thermal ellipsoids represent 30% probability. Solvent molecules are omitted for clarity.

Finally, we obtained single crystals of subporphyrin **6iB**, which revealed the structure as shown in Figure 6 (Table 5). The chiral unit cell (*P1* space group) contains two subporphyrins with the same chirality, but the packing structure is similar to that of **5i**.<sup>[16]</sup> The phenyl group is axially attached to the boron atom with a B–C bond length of 1.58 and 1.63 Å. The bowl depth is 1.34 Å, which is similar to those of axial methoxy forms.

## Summary

ABC-Type *meso*-aryl-substituted subporphyrins **5a–5j** were synthesized for the first time. Cooperative substituent effects are observed for donor–acceptor-type subporphyrins. Although the enantiomeric separation has not been successful for B-methoxy ABC-type subporphyrins, the enantiomers of B-phenyl-substituted subporphyrins **6f** and **6i** have been resolved by using chiral HPLC. These results suggest a facile racemization of B-methoxy ABC subporphyrins in solution, and also subporphyrins in general.

## Experimental Section

**5-(4-*tert*-Butylphenyl)-10-phenyltripyrane (4a)**: To a suspension of 1-benzoyl-5-(4-*tert*-butylphenyl)dipyrromethane (**3a**; 3.83 g, 10.0 mmol) and  $\text{NaBH}_4$  (10 equiv.) in dry tetrahydrofuran (THF; 100 mL), MeOH (10 mL) was added dropwise under  $\text{N}_2$ . When the reaction was over, the reaction was quenched with a saturated aqueous  $\text{NH}_4\text{Cl}$  solution, and the product was extracted with ethyl acetate. The organic phase was washed with brine, and dried with anhydrous  $\text{Na}_2\text{SO}_4$ . The solvent was evaporated, and the residue was dissolved in pyrrole (20 mL, 288 mmol). A solution of trifluoroacetic acid (TFA; 0.15 mL, 1.96 mmol) in  $\text{CH}_2\text{Cl}_2$  (1.5 mL) was added to the solution at 0 °C under  $\text{N}_2$ . The reaction mixture was stirred for 15 min, and then was quenched by addition of triethylamine (0.40 mL, 2.95 mmol). The solution was evaporated under reduced pressure, and the residue was purified by silica-gel column chromatography (eluent:  $\text{CH}_2\text{Cl}_2/n$ -hexane, 1:1). The solvent was evaporated, and the residue dried in a vacuum to afford **4a** as brownish yellow amorphous solids (1.79 g, 41%).

**5-(4-Methoxyphenyl)-10-phenyltripyrane (4b)** and **5-(4-bromophenyl)-10-phenyltripyrane (4c)** were prepared in a similar manner.

**Methoxo[5-(4-*tert*-butylphenyl)-10-(4-nitrophenyl)-15-phenylsubporphyrinato]boron(III) (5a)**: To a suspension of 5-(4-*tert*-butylphenyl)-10-phenyltripyrane (**4a**; 0.460 g, 1.06 mmol) in 1,2-dichlorobenzene (40 mL, 26.5 mm) was added triethylamine–borane (470  $\mu\text{L}$ , 3 equiv.), and the resulting mixture was heated at 150 °C for 2 h under an  $\text{N}_2$  atmosphere to give triethylamine–tri-*N*-tripyrromethene–borane in situ. The solution color changed from fluorescent yellowish to dark orange. The solution was then diluted to 10 mm in 1,2-dichlorobenzene (106 mL). After the addition of 4-nitrobenzoyl chloride (10 equiv.) dissolved in 1,2-dichlorobenzene through a syringe the solution was stirred for 30 min at 150 °C under  $\text{N}_2$ . The reaction mixture was quenched by addition of pyridine (12 equiv.), and the resulting solution was heated to reflux under aerobic conditions for 1 h. The solution was cooled to room temperature and ethylenediamine (10 equiv.) was added to the solution and the mixture was stirred for 1 h. Then, the solution was poured

Table 5. Crystal data of subporphyrins **5g–5j**, **6i** and **6iB**.

	<b>5g</b>	<b>5h</b>	<b>5i</b>
Formula	C <sub>33</sub> H <sub>24</sub> BN <sub>3</sub> O <sub>2</sub> S	(C <sub>34</sub> H <sub>21.9</sub> BBrN <sub>4</sub> O <sub>3</sub> ) <sub>2</sub> (C <sub>6</sub> H <sub>6</sub> ) <sub>3</sub>	C <sub>49</sub> H <sub>39</sub> BN <sub>4</sub> O <sub>2</sub>
FW	537.42	1484.65	726.65
Crystal system	monoclinic	triclinic	triclinic
Space group	<i>P</i> 2 <sub>1</sub> / <i>c</i> (no. 14)	<i>P</i> 1̄ (no. 2)	<i>P</i> 1̄ (no. 2)
<i>a</i> /Å	7.5286(1)	14.179(3)	10.1409(3)
<i>b</i> /Å	19.5441(4)	14.583(4)	11.8103(4)
<i>c</i> /Å	17.2428(3)	17.474(4)	15.9675(5)
<i>α</i> /°	90	87.480(19)	85.5185(18)
<i>β</i> /°	94.6863(12)	71.040(15)	81.5718(19)
<i>γ</i> /°	90	89.47(2)	77.5712(18)
<i>V</i> /Å <sup>3</sup>	2528.62(8)	3413.8(15)	1845.24(10)
<i>Z</i>	4	2	2
<i>T</i> /K	93	93	93
$\rho_{\text{calcd.}}$ /g cm <sup>-3</sup>	1.412	1.444	1.308
<i>R</i> <sub>1</sub> [ <i>I</i> > 2σ( <i>I</i> )]	0.0697	0.0884	0.0927
<i>R</i> <sub>w</sub> (all data)	0.2243	0.2088	0.2976
GOF	1.035	1.006	1.046
	<b>5j</b>	<b>6i</b>	<b>6iB</b>
Formula	C <sub>48</sub> H <sub>36</sub> BN <sub>5</sub> O <sub>3</sub> (C <sub>4</sub> H <sub>10</sub> O)	(C <sub>54</sub> H <sub>41</sub> BN <sub>4</sub> O) <sub>2</sub> (C <sub>6</sub> H <sub>6</sub> ) <sub>3</sub>	(C <sub>54</sub> H <sub>41</sub> BN <sub>4</sub> O) <sub>2</sub> (C <sub>6</sub> H <sub>6</sub> ) <sub>3</sub> (CO) <sub>0.81</sub>
FW	815.75	1007.04	1029.73
Crystal system	triclinic	triclinic	triclinic
Space group	<i>P</i> 1̄ (no. 2)	<i>P</i> 1̄ (no. 2)	<i>P</i> 1̄ (no. 2)
<i>a</i> /Å	12.38(1)	10.131(6)	10.152(3)
<i>b</i> /Å	13.401(10)	17.808(8)	18.232(4)
<i>c</i> /Å	13.944(10)	18.298(10)	18.267(4)
<i>α</i> /°	96.228(7)	110.61(8)	111.06(3)
<i>β</i> /°	111.405(19)	105.55(12)	103.39(4)
<i>γ</i> /°	98.06(3)	102.97(9)	104.91(5)
<i>V</i> /Å <sup>3</sup>	2107(3)	2785(5)	2845(2)
<i>Z</i>	2	2	2
<i>T</i> /K	93	93	93
$\rho_{\text{calcd.}}$ /g cm <sup>-3</sup>	1.286	1.201	1.202
<i>R</i> <sub>1</sub> [ <i>I</i> > 2σ( <i>I</i> )]	0.0707	0.630	0.813
<i>R</i> <sub>w</sub> (all data)	0.2201	0.1976	0.2302
GOF	1.090	1.009	1.068

onto a silica pad. Elution with CH<sub>2</sub>Cl<sub>2</sub> removed 1,2-dichlorobenzene, unreacted aryl chloride, and some byproducts. Then elution with MeOH/TFA (20:1) afforded a black fraction. The solution was neutralized by saturated aqueous NaHCO<sub>3</sub>, extracted with CH<sub>2</sub>Cl<sub>2</sub>, washed with 1 M HCl, and dried with anhydrous Na<sub>2</sub>SO<sub>4</sub>. MeOH was added to the solution and the mixture was heated at 50 °C. After 15 min the solvent was evaporated and the residue was purified by silica-gel column chromatography (eluent: CH<sub>2</sub>Cl<sub>2</sub>/*n*-hexane/EtOAc, 1:4:1). The yellow fraction of subporphyrin and the red fraction of subchlorin were carefully collected by checking with TLC. Subchlorins were converted into subporphyrins by MnO<sub>2</sub> oxidation. The solution was passed through a Celite pad to remove MnO<sub>2</sub>. After the B-OMe form of subporphyrins was converted into the B-OH form by washing with 1 M HCl, the solution was washed with NaHCO<sub>3</sub> aq., and dried with anhydrous Na<sub>2</sub>SO<sub>4</sub>. The solvent was evaporated and the residue was purified by silica-gel column chromatography (eluent: CH<sub>2</sub>Cl<sub>2</sub>/*n*-hexane/EtOAc, 1:4:1, followed by MeOH/TFA, 20:1). The solution was neutralized with saturated aqueous NaHCO<sub>3</sub>, extracted with CH<sub>2</sub>Cl<sub>2</sub>, washed by brine, and dried with anhydrous Na<sub>2</sub>SO<sub>4</sub>. MeOH was added to the solution and the mixture was heated at 50 °C to convert the B-OH form into the B-OMe form. The solvent was evaporated, and the residue was purified by silica-gel column chromatography (eluent: CH<sub>2</sub>Cl<sub>2</sub>/*n*-hexane/EtOAc, 1:4:1). Recrystallization from CH<sub>2</sub>Cl<sub>2</sub>/*n*-hexane afforded pure subporphyrins as orange solids (48.0 mg, 7.5%).

ABC-Type subporphyrins **5b–5h** were prepared in a similar manner.

CCDC-983700 (for **5g**), -983701 (for **5h**), -983702 (for **5i**), -983703 (for **5j**), -983704 (for **6i**), and -983705 (for **6iB**) contain the supplementary crystallographic data for this paper. These data can be obtained free of charge from The Cambridge Crystallographic Data Centre via [www.ccdc.cam.ac.uk/data\\_request/cif](http://www.ccdc.cam.ac.uk/data_request/cif).

**Supporting Information** (see footnote on the first page of this article): The Supporting Information for this article contains NMR spectra of all compounds; UV-Vis and fluorescence spectra of Subporphyrin **5a–5j**; X-ray Crystal structures of Subporphyrins **5g**, **5h**, and **5j**; An analysis of the crystal data of Subporphyrins **6i** (Racemic) and **6iB** (Enantiomeric Pure); and CD spectra for Subporphyrins **6iA** and **6iA** and the calculated CD spectra for Subporphyrin **6f**.

## Acknowledgments

This work was supported by the Japanese Ministry of Education, Culture, Sports, Science and Technology (MEXT) through Grants-in-Aid [grant number 25220802 (S)] for Scientific Research. The authors thank Daisel people (Mr. Miyamoto) for their help in finding conditions for the optical separation of subporphyrins. H. M.

acknowledges the Japan Society for the Promotion of Science (JSPS) for a Fellowship for Young Scientists.

- [1] a) Y. Inokuma, A. Osuka, *Dalton Trans.* **2008**, 2517; b) T. Torres, *Angew. Chem. Int. Ed.* **2006**, *45*, 2834; *Angew. Chem.* **2006**, *118*, 2900; c) A. Osuka, E. Tsurumaki, T. Tanaka, *Bull. Chem. Soc. Jpn.* **2011**, *84*, 679; d) C. G. Claessens, D. González-Rodríguez, M. S. Rodríguez-Morgade, A. Medina, T. Torres, *Chem. Rev.*, DOI: 10.1021/cr400088w.
- [2] Y. Inokuma, J. H. Kwon, T. K. Ahn, M.-C. Yoo, D. Kim, A. Osuka, *Angew. Chem. Int. Ed.* **2006**, *45*, 961; *Angew. Chem.* **2006**, *118*, 975.
- [3] a) N. Kobayashi, Y. Takeuchi, A. Matsuda, *Angew. Chem. Int. Ed.* **2007**, *46*, 758; *Angew. Chem.* **2007**, *119*, 772; b) Y. Takeuchi, A. Matsuda, N. Kobayashi, *J. Am. Chem. Soc.* **2007**, *129*, 8271.
- [4] Y. Inokuma, Z. S. Yoon, D. Kim, A. Osuka, *J. Am. Chem. Soc.* **2007**, *129*, 4747.
- [5] a) Y. Inokuma, S. Easwaramoorthi, S. Y. Jang, K. S. Kim, D. Kim, A. Osuka, *Angew. Chem. Int. Ed.* **2008**, *47*, 4840; *Angew. Chem.* **2008**, *120*, 4918; b) Y. Inokuma, S. Easwaramoorthi, Z. S. Yoon, D. Kim, A. Osuka, *J. Am. Chem. Soc.* **2008**, *130*, 12234.
- [6] T. Tanaka, M. Kitano, S. Hayashi, N. Aratani, A. Osuka, *Org. Lett.* **2012**, *14*, 2694.
- [7] M. Kitano, S. Hayashi, T. Tanaka, H. Yorimitsu, N. Aratani, A. Osuka, *Angew. Chem. Int. Ed.* **2012**, *51*, 5593; *Angew. Chem.* **2012**, *124*, 5691.
- [8] a) D. M. Wallace, K. M. Smith, *Tetrahedron Lett.* **1990**, *31*, 7265; b) C.-H. Lee, F. Li, K. Iwamoto, J. Dadok, A. A. Bothner-By, J. S. Lindsey, *Tetrahedron* **1995**, *51*, 11645; c) P. D. Rao, S. Dhanalekshmi, B. J. Littler, J. S. Lindsey, *J. Org. Chem.* **2000**, *65*, 7323; d) D. K. Dogutan, S. H. H. Zaidi, P. Thamyongkit, J. S. Linsey, *J. Org. Chem.* **2007**, *72*, 7701; e) M. O. Senge, Y. M. Shaker, M. Pinteá, C. Ryppa, S. S. Hatscher, A. Ryan, Y. Sergeeva, *Eur. J. Org. Chem.* **2010**, 237; f) J. S. Lindsey, *Acc. Chem. Res.* **2010**, *43*, 300; g) M. O. Senge, *Chem. Commun.* **2011**, 47, 1943.
- [9] a) S. Hayashi, Y. Inokuma, S. Easwaramoorthi, K. S. Kim, D. Kim, A. Osuka, *Angew. Chem. Int. Ed.* **2010**, *49*, 321; *Angew. Chem.* **2010**, *122*, 331; b) S. Hayashi, Y. Inokuma, A. Osuka, *Org. Lett.* **2010**, *12*, 4148.
- [10] A. Szumna, *Chem. Soc. Rev.* **2010**, *39*, 4274.
- [11] a) C. G. Claessens, T. Torres, *Tetrahedron Lett.* **2000**, *41*, 6361; b) S. Shimizu, A. Miura, S. Khene, T. Nyokong, N. Kobayashi, *J. Am. Chem. Soc.* **2011**, *133*, 17322; c) I. Sánchez-Molina, B. Grimm, R. M. K. Calderon, C. G. Claessens, D. M. Guldi, T. Torres, *J. Am. Chem. Soc.* **2013**, *135*, 10503.
- [12] S. Higashibayashi, H. Sakurai, *J. Am. Chem. Soc.* **2008**, *130*, 8592.
- [13] C. Thilgen, F. Diederich, *Chem. Rev.* **2006**, *106*, 5049.
- [14] a) E. M. Pérez, N. Martín, *Org. Biomol. Chem.* **2012**, *10*, 3577; b) C. Wang, K. Takei, T. Takahashi, A. Javey, *Chem. Soc. Rev.* **2013**, *42*, 2592.
- [15] S. Saga, S. Hayashi, K. Yoshida, E. Tsurumaki, P. Kim, Y. M. Sung, J. Sung, T. Tanaka, D. Kim, A. Osuka, *Chem. Eur. J.* **2013**, *19*, 11158.
- [16] In this paper we do not discuss the absolute configuration of **6iB** because; (i) the CD spectrum is very weak and we could not obtain distinct mirror-image CD signals, and (ii) the X-ray diffraction data of **6iB** can not be used to determine the absolute configuration for this molecule owing to the absence of heavy atoms.

Received: April 17, 2014  
Published Online: May 27, 2014